Proposal for J-PARC 50 GeV Proton Synchrotron

Study of in medium mass modification for the ϕ meson using ϕ meson bound state in nucleus

submitted on 16/June/2009

P. Bühler[1], C. Curceanu[2], C. Guaraldo[2], O. Hartmann[1], K. Hicks[3], M. Iwasaki[4,5], T. Ishiwatari[1], P. Kienle[6], J. Marton[1], R. Muto[7], M. Niiyama[4], H. Noumi[8], H. Ohnishi[4] †, S. Okada[2], A. Romero Vidal[2], A. Sakaguchi[9], F. Sakuma[4], S. Sawada[7], D. Sirghi[2], F. Sirghi[2], K. Suzuki[1], D.J. Tedeschi[10], K. Tsukada[4], O. Vazquez Doce[2], E. Widmann[1], S. Yokkaichi[4] and J. Zmeskal[1]

[1] *Stefan Meyer Institute for Subatomic Physics, Vienna, Austria*
[2] *Laboratori Nazionali di Frascati dell' INFN, Italy*
[3] *Department of Physics and Astronomy, Ohio University, Athens, Ohio 4571, USA*
[4] *RIKEN Nishina Center, RIKEN, Japan*
[5] *Tokyo Institute of Technology, Japan*
[6] *Technische Universiat Munchen, Germany*
[7] *KEK (High Energy Accelerator Research Organization), Japan*
[8] *Research center for Nuclear Physics (RCNP), Osaka University, Japan*
[9] *Department of Physics, Osaka University, Toyonaka, Osaka 560-0043, Japan*
[10] *Department of Physics and Astronomy University of South Carolina Columbia, SC 29208*

Abstract

We propose to study in-medium mass modification of the ϕ meson via the formation of ϕ meson bound state. We demonstrate that a completely background-free missing-mass spectrum can be obtained efficiently by $(\overline{p}, \phi)$ spectroscopy together with the $K^+\Lambda$ tagging, using the primary reaction channel $\overline{p}p \to \phi\phi$. From both missing mass and invariant mass study of the sub-threshold energy region, one can independently deduce the mass shift information. A systematic study over several nuclear targets will yield a unique, definitive and precise determination of the in-medium mass modification of the vector meson $\phi(s\overline{s})$.

†spokesperson : h-ohnishi@riken.jp

Contents

1 Introduction

A proton is composed of two 'Up' quarks and one 'Down' quark and having mass of 938 MeV/c^2. On the other hand, mass of bear quark, *i.e.* 'Up' and 'Down' quark are known to be a few MeV. Therefore, contribution of the constituent quarks to the mass of the proton is only a few % at most. The question need to be answered is the mechanism to generate more than 90% of the proton mass from vacuum. This mechanism is now known as spontaneous breaking of chiral symmetry, which create non zero $\langle\overline{q}q\rangle$ expectation value in vacuum. This $\langle\overline{q}q\rangle$-condensation is the major source of masses of low lying hadrons such as protons, neutrons, pions, *etc.* In the theoretical framework, the $\langle\overline{q}q\rangle$ expectation value (chiral order parameter) is a function of temperature and chemical potential (density).

Various experimental studies have been performed to detect the restoration of the chiral symmetry. One of the approach is invariant mass spectroscopy of di-leptons from both hot/dense and normal nuclear matter. The other is formation of meson nucleus bound state and measures energy level of the state itself.

An important results was presented from invariant mass spectroscopy of di-muons in hot and/or dense nuclear media created by high energy heavy ion collisions at CERN-SPS[1]. The result was shown in Figure 1. The experiment claimed that significant modification of ρ meson spectra function under the condition of hot nuclear matter which indicates the ρ meson property modification under the extreme condition such as high template.

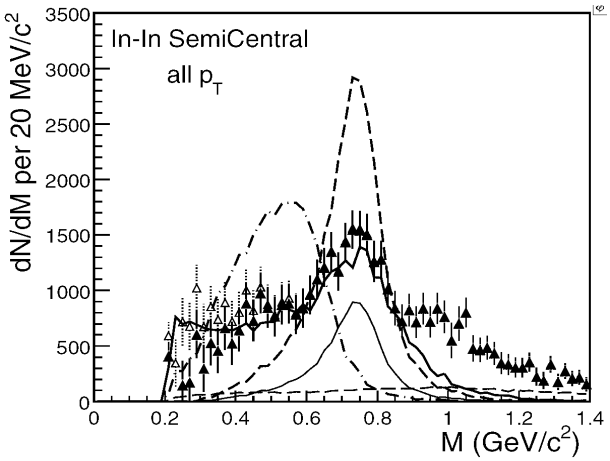

Figure 1: The invariant mass spectra of $\mu^+\mu^-$ at CERN NA60 [1].

The other important result is the invariant mass spectrum of $\phi \to e^+e^-$ using $p+A$ reactions with 12 GeV protons by the KEK-PS experiment E325 [2]. Figure 2 shows the invariant mass spectrum of $\phi \to e^+e^-$, and an excess on the low-mass side of the ϕ meson peak was observed in the low $\beta\gamma$ ($\equiv p/m$) region of ϕ mesons ($\beta\gamma < 1.25$) with copper targets. However, in the high $\beta\gamma$ region ($\beta\gamma > 1.25$), spectral shapes of ϕ mesons were consistent with the Breit-Wigner shape, *i.e.*, spectrum shape in vacuum. Since the mass modification of the ϕ mesons in a target nucleus is expected to be visible only for slow ϕ mesons produced in a heavy target nucleus, they concluded that the excess is considered to be the signal of the mass modification of the ϕ mesons in a target nucleus. To interpret the invariant mass spectra of ϕ mesons measured in the E325 experiment, the simplest approach is to assume that the spectrum shape of ϕ meson is modified in the nuclear medium. This allows us to compare the spectrum directly to the theoretical predictions. There are a number of predictions about the mass shift of ϕ mesons in nuclei, from QCD calculations such as the Brown-Rho scaling [3], the QCD sum-rule [4, 5], the effective chiral Lagrangian [6], the renormalization of the kaon [7], *etc.* The comparison based on a simple model calculation gives about 3 %

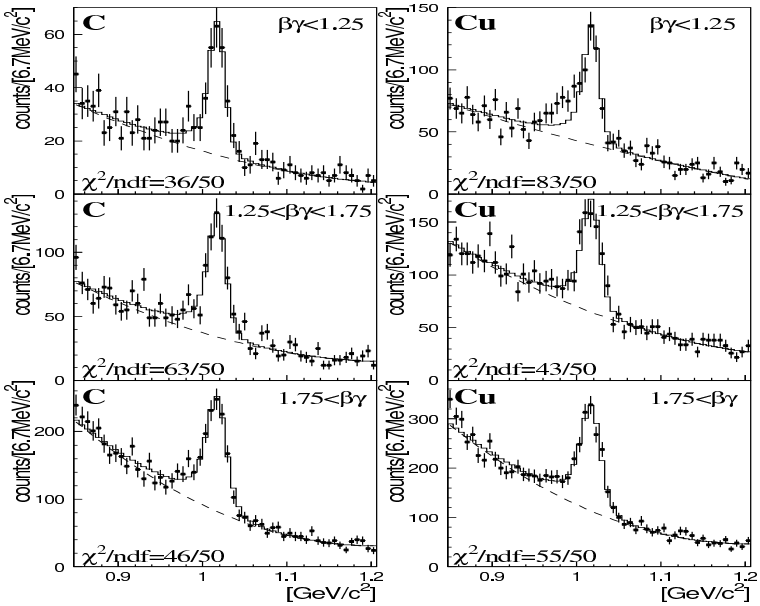

Figure 2: The invariant mass spectra of $\phi \to e^+e^-$ at KEK-PS E325 [2].

mass reduction and 3.4 times width broadening of the ϕ in nuclear media [2]. On the other hand, there is criticism of such a straightforward comparison of the invariant mass [8]. Therefore the conclusion that properties of the in-medium ϕ meson have been modified is still controversial.

Another Experimental approach to access the information of partial restoration of the chiral symmetry in the nuclear media via meson embedded in the nucleus has been performed and in progress. One milestone of the study using mesons is the observation of deeply-bound pionic atom states in nuclei [9, 10]. Results are shown in Figure 3. In the pionic atom case, the Bohr radius of the pion in heavy nuclei lies within the nucleus, but the s-wave strong interaction of the pion is repulsive so the major part of the wave function is pushed away from the nucleus, and the pions are bound to the nuclear surface by the Coulomb force. Through the study of the energy shift and width of the state, there is an indication of chiral symmetry restoration through the in-medium modification of the pion decay constant, f_π, leading to a proposed systematic study at RIBF (RIKEN Nishina Center).

Kaonic nuclear bound states provide another channel for the study of chiral symmetry. A recent hot topic concerns the possible existence of a deeply bound kaonic nuclear state. In this case, the $\overline{K}N$ interaction is expected to be strongly attractive, so the change in properties of the medium itself, and not just the meson, could be studied. Some of the results are shown in Figure 4. There are several experimental searches of the state [11, 12, 13, 14], although clear and definitive experimental evidence is still missing. An experimental study, J-PARC E15, is now being prepared to search for the simplest system, "K^-pp", by the in-flight (K^-, n) method.

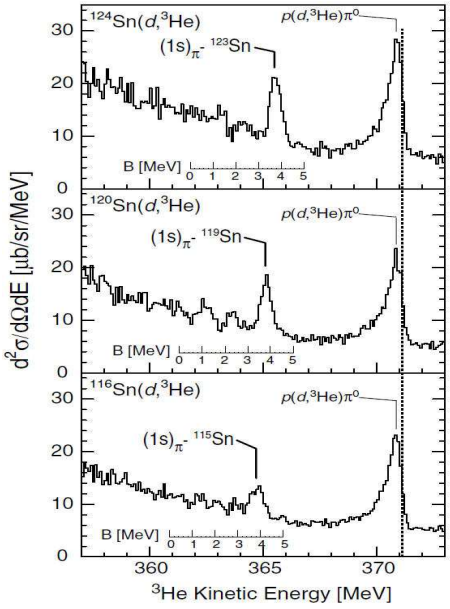

Figure 3: Double differential cross section as a function of ^{3}He kinetic energy of ^{124,120,116}Sn(d,^{3}He) reaction.[10]

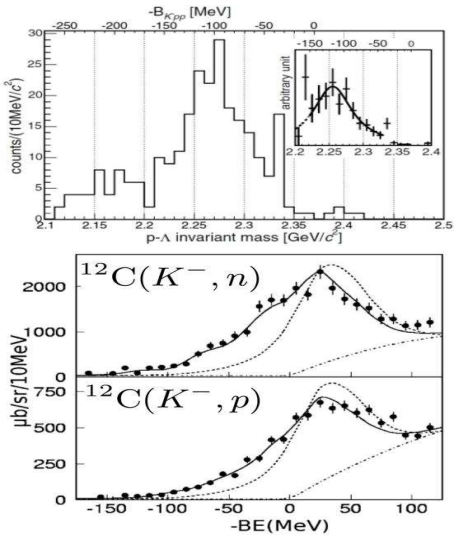

Figure 4: Top: Back-to-back Λp invariant mass spectra from K^- absorption reaction on ^{6}Li target.[13]. Bottom: Missing mass spectra for ^{12}C(K^-,n) and ^{12}C(K^-,p) reaction shown in Reference[14].

2 Goal of the proposed experiment

In this proposed experiment, we will focusing on the property of the ϕ meson in nuclear media.

As we discussed in previous section, experimental study of ϕ meson invariant mass spectra in the pA reaction reported that the ϕ meson mass shift in medium-heavy nuclei (Cu) is about 3 % and the natural width broadening of $\Gamma_\phi/\Gamma_\phi^{free} \approx 3.4$ [2].

Theoretically, in-medium mass shift of the ϕ meson at normal nuclear density is predicted to be $\Delta m_\phi/m_\phi = 1.5 \sim 2.6\%$ by the QCD sum rule as shown in figure 5 (left) [5]. For the width of the ϕ meson, there are several theoretical predictions and the predicted widths are quite narrow. Klingl-Waas-Weise predicted that the width is below $\Gamma_\phi < 10$ MeV [15], while Oset-Ramos reported that the width can be bigger, $\Gamma_\phi < 16$ MeV (for $\Delta m_\phi \sim 30$ MeV/c^2), taking into account Σ^* and the vertex correction in the chiral unitary model [16] (figure 5 (right)). All the currently available theoretical predictions give a quite narrow natural decay width of the ϕ even in the nuclear medium.

These numbers are in quite good agreement between experimental results and theoretical predictions, except for the strength of the attraction of the chiral unitary model. The interaction obtained by Oset-Ramos is attractive [16], but much weaker than what one can expect from reference [5].

To conclude the strength of the ϕ meson mass shift in nuclear media, definitely we need to perform new generation of the experiment. There are two possible ways to

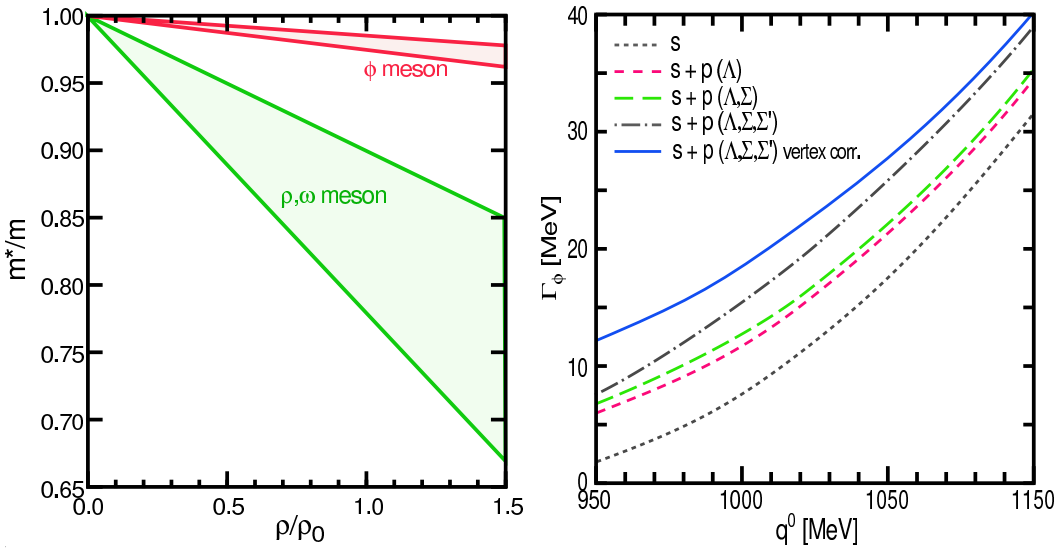

Figure 5: Theoretical calculation of the in-medium mass shift of the ϕ by the QCD sum rule (left) [5], and the in-medium decay width by using the chiral unitary model (right) [16].

approach the problem. One is precise measurement of the di-electron spectra via p-A collisions at J-PARC with 100 times more statistics than previous experiment at KEK, which is now in preparation as J-PARC E16 experiment[17].

The other way is that trying to produce only slowly moving ϕ meson where the maximum nuclear matter effect can be probed. One of the extreme condition can be achieved in laboratory is indeed formation of ϕ-nucleus bound state, where ϕ meson is "trapped" in nuclear media.

The purpose of the proposed experiment is to search for the ϕ-nucleus bound state and measured the binding energy of the system. The measurement must be done with different target nucleus to see the evolution of binding energy of newly generated nuclear cluster, ϕ-nucleus bound state.

3 Experimental method

For this proposed experiment, we are going to identify ϕ meson bound state by missing mass approach using $p(\overline{p},\phi)\phi$ reaction. The big advantage for this elementary process is that, in principle, we will be able to perform almost background free experiment when we detect four strangeness particles in final state. In the following subsections, first of all, we will present why we choose $p(\overline{p},\phi)\phi$ reaction as a elementary process for this experiment and after words, detail experimental method will be discussed.

3.1 The ϕ meson production via ($\overline{p}$, ϕ) reactions

3.1.1 Production cross section

To search for gluonic matter and exotic quark-gluon formations, intensive studies have been performed at the CERN/LEAR facility for the "OZI-forbidden" formation reaction of the type $\overline{p}p \to M_1 M_2$, where M_1 and M_2 are vector mesons. One striking result is the rather large $\phi\phi$ production cross section near the production threshold ($\sim$ 0.9 GeV/c), namely incident $\overline{p}$ momentum at around 1.3 $\sim$ 1.4 GeV/c[18]. Figure 6 (left) shows the production cross section for double ϕ meson production as a function of incident momentum for $\overline{p}$ together with direct production of ϕ K^+K^- and $K^+K^-K^+K^-$ (non-resonant $K\overline{K}$ pairs).

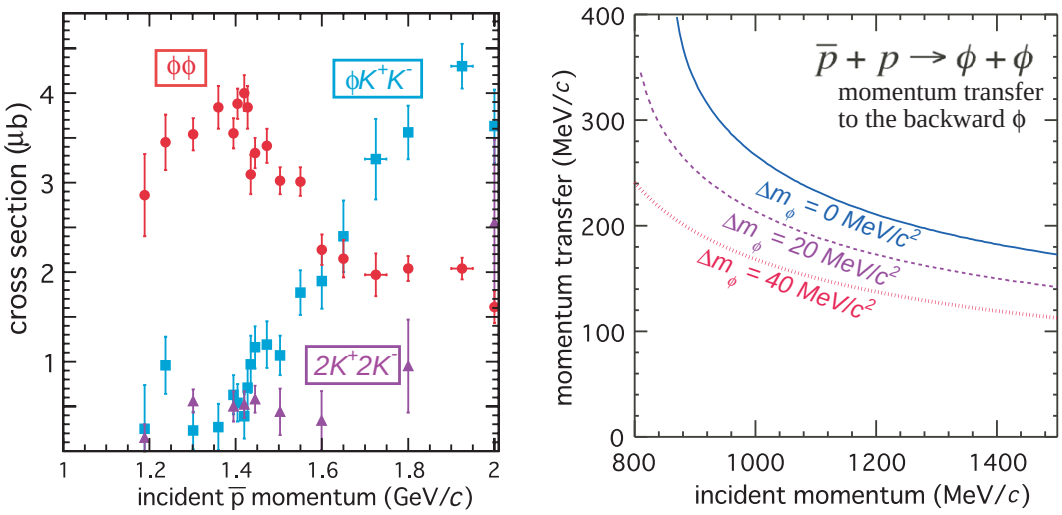

Figure 6: Left panel shows the cross section for double ϕ meson production around the production threshold [18]. Right panel shows the momentum transfer for backward ϕ production as a function of the incident $\overline{p}$ momentum.

The cross section of the double-ϕ channel has a peak at around a $\overline{p}$ momentum of 1.3 $\sim$ 1.4 GeV/c. In this momentum region, other kaon associated reactions, ϕK^+K^- and $K^+K^-K^+K^-$, have considerably lower cross sections ($\sim$ 10 %) as shown in figure 6 (left), in spite of their lower Q-values. This reaction is indeed appropriated for the missing mass spectroscopy for ϕ meson bound state, because when we detect ϕ meson in this reaction at the incident $\overline{p}$ momentum less than 1.4 GeV/c ensured the other ϕ meson produced.

3.1.2 Missing mass spectroscopy

Let us focus on the double-ϕ elementary reaction channel. In this reaction, one can use the backward ϕ as the source of the quasi-recoilless ϕ meson production channel,

and the forward ϕ as a spectroscopic analyzer of the missing mass of the backward ϕ-mesonic nuclei.

The incident ($\overline{p}$, ϕ) reaction can be written as,

$$\overline{p} + {}^{A+1}_{Z+1}\mathrm{X}' \rightarrow \{\phi\ {}^{A}_{Z}\mathrm{X}\} + \phi. \tag{1}$$

Therefore missing mass can be described as

$$M_{missing} = M_{{}^{A}_{Z}\mathrm{X}} + m_{\phi} - B_{\phi}, \tag{2}$$

where $M_{{}^{A}_{Z}\mathrm{X}}$ is the mass of the residual (spectator) nucleus ${}^{A}_{Z}\mathrm{X}$. If $\{\phi\ {}^{A}_{Z}\mathrm{X}\}$ is formed, the missing mass $M_{missing}$ should be located below the threshold energy $M_{{}^{A}_{Z}\mathrm{X}} + m_{\phi}$.

For these channels, the missing masses of the ϕ mesonic nuclei $\{\phi\ {}^{A}_{Z}X\}$ and their rest frames can be obtained by the forward ϕ meson momentum using $\phi \rightarrow K^{+}K^{-}$ decay.

3.1.3 The momentum transfer of the reaction

The momentum transfer of the reaction is shown in figure 6 (right). As shown in the figure, the momentum transfer to the backward ϕ is monotonically decreasing as a function of incident $\overline{p}$ beam momentum from $|q|$ $\sim$240 MeV/c at 1.1 GeV/c and below 180 MeV/c at around 1.3 $\sim$ 1.4 GeV/c, where the double-ϕ cross section is maximum. It should be note that Fermi momentum of the nucleon in nucleus is $\sim$ 270 MeV/c which is almost same order of magnitude with the ϕ meson produced in ($\overline{p}$, ϕ) reactions, therefore ϕ bound-state formation rate would be possible. Let us consider the ratio of the bound state formation $R_{capture}$. A rough estimation is that $R_{capture} \sim \exp(-\mathbf{q}^2/{p_F}^2)$, where $\mathbf{q}$ is the momentum transfer to the ϕ meson. The formula represents the overlap integral between a plane wave of ϕ at the momentum of $\mathbf{q}$, and the ϕ wave function in the sub-threshold region. If we assume $|\mathbf{q}| \sim 240$ MeV/c, then the relative capture rate $R_{capture} \sim \exp(-\mathbf{q}^2/{p_F}^2) = 0.45$ at $p_F \sim 270$ MeV/c.

3.2 ϕ meson in nuclear media

What happens if a ϕ is in a nucleus? One can naturally expect that six $\phi N \rightarrow KY$ channels will open. Table 1 shows a summary of possible decay / reaction channels. In the table, the binding energy of the proton ("p") and neutron ("n") in a nucleus is expressed as B_p and B_n, respectively. Because the partial decay widths to each KY channel are not given in reference [16], we computed the branching ratio from the given partial widths of $K\Lambda$ and $K\Sigma$ channels, by assuming the isospin relation 1 : 2 between $K^0\Sigma^0$ and $K^+\Sigma^-$ channels, and that ϕp and ϕn have the same coupling strength.

The free-space decay channel is easy to analyze using the quasi-invariant mass, but it is difficult to observe. The di-lepton channel has a quite small branching ratio $\sim 10^{-4}$. Because of the small Q value, the $K\overline{K}$ channel is also difficult to observe if the

initial channel	decay/KY channel	branching ratio (%) $^{(*)}$	Q-value (MeV)
ϕ "p"	K^+ Λ	37	$348 - B_\phi - B_p$
	K^+ Σ^0	1	$271 - B_\phi - B_p$
	K^0 Σ^+	2	$275 - B_\phi - B_p$
	K Σ^* *etc.*	10	–
ϕ "n"	K^0 Λ	37	$346 - B_\phi - B_n$
	K^0 Σ^0	1	$269 - B_\phi - B_n$
	K^+ Σ^-	2	$268 - B_\phi - B_n$
	K Σ^* *etc.*	10	–

Table 1: Decay / reaction channels of the ϕ in nuclei. $(*)$: The decay branch is calculated from the theoretical partial widths contributed from $K\Lambda$ and $K\Sigma$ channels given in reference [16].

ϕ is produced near or below the threshold. At the threshold, the $K\overline{K}$-pair produced at around 126 MeV/c can easily stop around the target.

Therefore, let us focus on the KY decay channel of the ϕ mesonic nuclei, ignoring the effect of the final state interaction (FSI) for simplicity. Especially, the $K^+\Lambda$ channel is quite promising, not only because of its large branching ratio but also because of the large $p\pi^-$ decay branch (as much as 60%) of the Λ. This means that a large fraction of the channel can be reconstructed by measuring only charged particles. Unfortunately, observation of the $K^+\Sigma$ channel is difficult not only from its small branching ratio, but also because 1) the $\Sigma\Lambda$ conversion is known to be quite strong and 2) most of the charged-Σ decays emit neutral particles.

In a nucleus, the $K^+\Lambda$ channel can be observed as

$$\{\phi\ {}^{A}_{Z}\mathrm{X}\} \rightarrow K^+ + \Lambda + {}^{A-1}_{Z-1}\mathrm{X}'', \tag{3}$$

in which a ΛK^+ pair is produced by the simple quark re-configuration as

$$\phi(s\bar{s}) + \text{"}p\text{"}(uud) \rightarrow K^+(u\bar{s}) + \Lambda(uds). \tag{4}$$

If the ϕ is in a bound state or low momentum region (roughly below proton Fermi motion), then the ΛK^+ pair should be produced in a *back-to-back* direction at the center-of-mass (CM) of the $\{\phi\ {}^{A}_{Z}X\}$ system, because the kinetic energy of the ϕ is well below the Q-value. If we neglect the kinetic energy carried out by residual nuclei, then the invariant mass should be given as

$$m_{inv}(\Lambda K^+) \approx \sqrt{(m_\phi - \Delta m_\phi)^2 + \mathbf{p}^2_{cm'}} + \sqrt{m_p^{\mathrm{eff}\,2} + \mathbf{p}^2_{cm'}} \tag{5}$$

where m_ϕ and m_p are the mass of the ϕ and proton, respectively, $\mathbf{p}_{cm'}$ is the three-momentum of the ϕ (or proton) in the center of mass of the ϕ-p sub-system in $\{\phi\ {}^{A}_{Z}\mathrm{X}\}$,

$\Delta m(\phi)$ is the mass shift, and $m_p^{\rm eff}$ is the effective mass of the proton. If $p_{cm'}$ is small, it can be simplified as

$$m_{inv}(\Lambda K^+) \approx m_\phi + m_p - \Delta m_\phi - V_p + \langle \frac{m_\phi + m_p}{2 m_\phi m_p} \mathbf{p}^2_{cm'} \rangle, \tag{6}$$

where V_p is the real part of the optical potential of the proton.

Very unfortunately, there is no good way to deduce $\mathbf{p}_{cm'}$ experimentally. Thus, the invariant mass study of the ΛK^+-pair is even more difficult than that of the free decay mode of the ϕ. The invariant mass will be smeared out not only from the imaginary part, but by the internal kinetic term which is roughly 40 MeV, if we assume $|\mathbf{p}_{cm'}|$ is of the order of the Fermi-motion ~ 270 MeV/c. However this invariant mass is useful for defining an energy window to identify the ϕ production in the reaction using a rather wide window to cover the smearing effect.

3.3 Q-value of the ϕ mesic nucleus system

If one knows the rest frame of the ϕ mesic nucleus, and if it decays to three bodies $\{\phi\ {}^{A}_{Z}\mathrm{X}\} \rightarrow \Lambda + K^+ +\ {}^{A-1}_{Z-1}\mathrm{X}''$, then the Q-value can be given as

$$\begin{aligned} Q &= (m_\phi - B_\phi) + (m_p - B_p) - (m_{K^+} + m_\Lambda) \\ &= T_\Lambda + T_{K^+} + T_{{}^{A-1}_{Z-1}\mathrm{X}''}, \end{aligned} \tag{7}$$

where $\langle T_\Lambda \rangle$, $\langle T_{K^+} \rangle$ and $\langle T_{{}^{A-1}_{Z-1}\mathrm{X}''} \rangle$ are the kinetic energy of the final state Λ, K^+ and the residual nucleus (with proton hole), respectively. So thus

$$\begin{aligned} Q + m_{K^+} + m_\Lambda &= E^{rf}_\Lambda + E^{rf}_{K^+} + \frac{\mathbf{p}^2_{\Lambda K^+}}{2 M_{{}^{A-1}_{Z-1}\mathrm{X}''}} \\ &= m_\phi + m_p - B_\phi - B_p, \end{aligned} \tag{8}$$

where $M_{{}^{A-1}_{Z-1}\mathrm{X}^{"}}$ is the mass of the residual nucleus. E^{rf}_Λ and $E^{rf}_{K^+}$ are the total energy of Λ and K^+ in the rest frame of $\{\phi\ {}^{A}_{Z}\mathrm{X}\}$, and $\mathbf{p}_{\Lambda K^+}$ is the three-momentum of the ΛK^+-pair in the rest frame. All the quantities used to compute Q-value can be observed experimentally, thus this is an extremely interesting quantity for deducing B_ϕ, if one can define the frame by knowing the production channel. Note that formula (8) is obtained simply from energy conservation.

3.4 Experimental approach for the proposed experiment

As discussed, both Λ and K^+ are tagged with strangeness, thus with a loose cut for ΛK^+ invariant mass and by requiring *back-to-back* Λ and K^+ emission, we can expect a clear missing mass spectrum. From the missing mass, one can also select events which correspond to a specific ϕ-bound-state formation. It is also possible to extend

the study further, using formula (2) and (8) to check the consistency of the resultant binding energy. Namely, from a missing mass study of the ground state of the ϕ,

$$B_\phi = -\left(M_{missing} - M_{{}^A_Z\mathrm{X}} - m_\phi\right), \tag{9}$$

and from the energy conservation rule in the rest frame of $\{\phi\ {}^A_Z\mathrm{X}\}$,

$$B_\phi = -\left(E^{rf}_\Lambda + E^{rf}_{K^+} + \frac{\mathbf{p}^2_{\Lambda K^+}}{2M_{{}^{A-1}_{Z-1}\mathrm{X}''}} - m_\phi - m_p + B_p\right), \tag{10}$$

where ${}^A_Z\mathrm{X}$ is the core nucleus of the ϕ mesic nucleus $\{\phi\ {}^A_Z\mathrm{X}\}$, and ${}^{A-1}_{Z-1}\mathrm{X}''$ is the residual nucleus of the decay. Note that the mass $M_{{}^A_Z\mathrm{X}}$ and the proton binding energy B_p are not unique, but can be assigned if the width broadening of the ϕ bound state is relatively small. As described, one can deduce the mass shift of the ϕ meson in the nuclear medium by a systematic study of the ϕ bound states as

$$\Delta m_\phi = \left(1 - \left(\frac{A}{A^0_\phi}\right)^{-\alpha_\phi}\right)^{-1} B_\phi, \tag{11}$$

where A is the mass number of the nucleus and A^0 is the critical mass number for the ϕ to bind.

There are several remarkable points, which can be summarized as,

- decay channel, Λ and K^+, open only when ϕ is in a nucleus,
- both Λ and K^+ are labelled by strangeness coming from the $s\bar{s}$-pair of the ϕ,
- all charged final states in $\Lambda \to p\pi^-$ and K^+ makes for efficient detection,
- FSI effect should be minimized for the *back-to-back* condition,
- background-free missing-mass spectrum is expected, and
- ϕ mass shift can be detected by two independent methods.

Even if the branching ratio for the decay mode of $K^+\Sigma^0$ is small, there is a question whether the $K^+\Sigma^0$ channel could arise in the event if one could not detect the γ-ray emission of the Σ^0 decay $\Sigma^0 \to \gamma\Lambda$ ($BR \sim 100\%$). It should be noted that $K^+\Lambda$ invariant mass spectrum will be shifted by 70 MeV for the events from $K^+\Sigma^0$ if experimental detector is not sensitive to the neutral particles, *i.e.* missing γ ray from Σ^0 decay. However, if the overall energy resolution for the detector is better than 70 MeV, we can separate the $K^+\Sigma^0$ events from the $K^+\Lambda$ direct decay events.

3.5 Physical background

Let us consider how to ensure that the backward ϕ is in a nucleus. As discussed, we can tag the events which have *back-to-back* ΛK^+-pair production at the momentum region around 200 $\sim$ 600 MeV/c for both Λ and K^+, whose quasi-invariant mass is in the region of interest. By this tagging, we can select the cascade reactions $\overline{p}+{}^{A+1}_{Z+1}\mathrm{X}' \rightarrow \{\phi\ {}^{A}_{Z}\mathrm{X}\} + \phi$ and $\{\phi\ {}^{A}_{Z}\mathrm{X}\} \rightarrow {}^{A-1}_{Z}\mathrm{X}'' + \Lambda + K^+$.

As we discussed already in previous sections, the most distinguishable feature of this reaction channel is its fully background-free nature. The yield of the kaon-associated ϕ production channel, ϕK^+K^- and $K^+K^-K^+K^-$, is much smaller than the double ϕ production channel for the incident $\overline{p}$ momentum below 1.4 GeV/c, and those events can be discriminated by the invariant mass analysis so no background processes exist in the primary reaction. Another unique feature is that all the particles we shall observe, including forward $\phi \rightarrow K^+K^-$ decay, are labeled with strangeness so the discrimination from other processes is quite clear, which ensures that it is free from any accidental background formation.

However, the hardware trigger for these events is difficult. Figure 7 shows cross sections of possible sources which may create fake hardware trigger as a function of incident $\overline{p}$ momentum. For this experiment, the forward ϕ meson can be detected with a K^+K^- pair. Therefore, efficient trigger and detection of forward going K^+K^- is essential. As we can see in figure 7, if we could select two Kaons efficiently, possible major source of background, like multi-pion production, which makes fake trigger in hardware level will be suppressed. The number of expected fake trigger rate will be discussed in the next section.

4 Experimental apparatus

As shown in Figure 6, a quasi-recoilless condition (below typical Fermi motion in nuclei) for the reaction can be achieved for the incident $\overline{p}$ momentum more than 1.0 GeV/c. It has been already discussed in Section 3.1.1, to minimise major physical background, such as $\overline{p} + p \rightarrow KKKK$ or ϕKK, the experiment must be performed with incident $\overline{p}$ momentum below 1.5 GeV/c where expected production cross section of double ϕ meson is about a few μb.

The momentum of the ϕ meson from the double ϕ meson production with 1.1 GeV/c incident $\overline{p}$ beam momentum on a proton target is plotted in figure 8 (left). In the case of nuclear target, only extremely forward ϕ meson production events, having momentum around 0.9 GeV/c, contribute to the ϕ meson bound state formation by the backward ϕ meson. This is different from the proton target case, in which ϕ meson momentum is quite sensitive to the production angle as shown in figure 8 (left). The decay K^+K^- which form this forward ϕ have momenta around 400 MeV/c as shown in figure 8 (right). The opening angles from the beam axis of the charged kaons are rather large - about 0.25 rad.

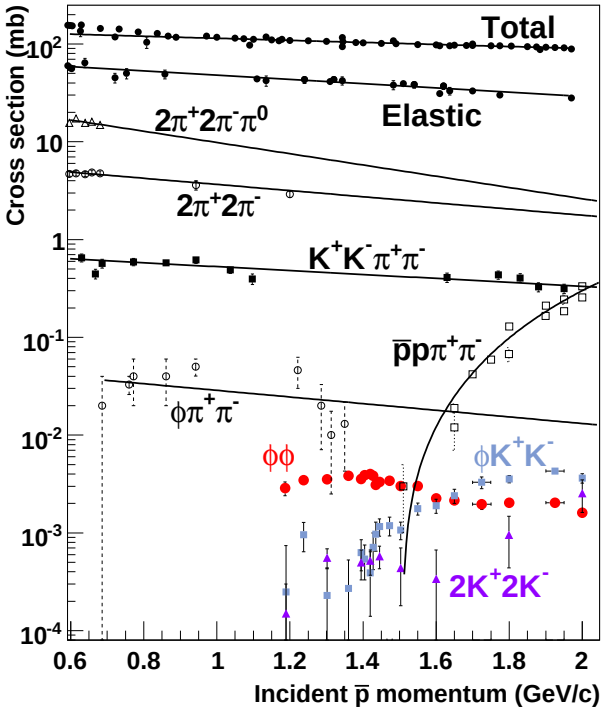

Figure 7: Cross section of various $\overline{p}p$ reaction branches as a function of incident momentum of $\overline{p}$.

The experimental setup consists of 3 major parts. First one is the beam line spectrometer which identifies particle species and analyzes incident beam momentum. Second component is large solid angle tracking detector for both K^+K^- pair from forward going ϕ meson decay and decayed K^+ and Λ from bound state together with Time of Flight wall to identify $K^\pm$ in offline analysis. Third one is trigger cherenkov counter for forward going Kaons.

In the following subsections, detail description for the those three components are1.1 GeV/c discussed.

4.1 Beam line spectrometer

A part of beam line magnets together with beam tracker, anti-proton identification detector and time zero detector will be main components of the beam line spectrometer.

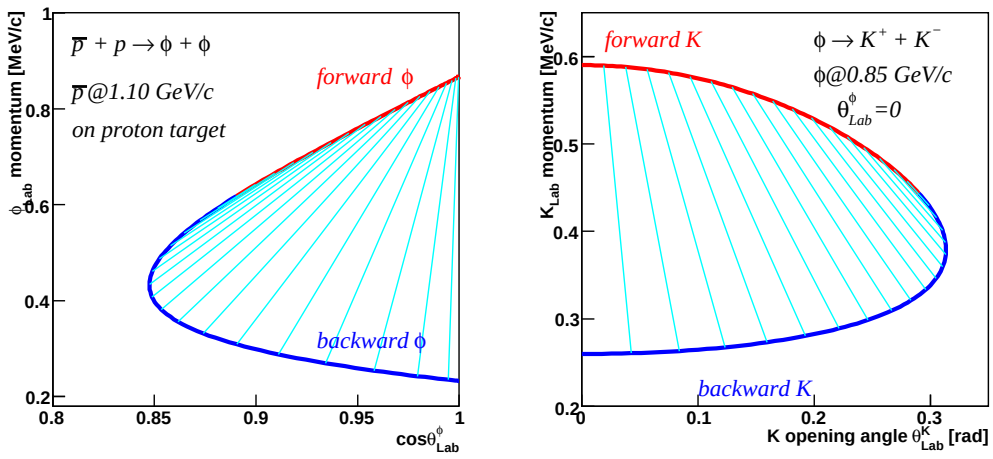

Figure 8: Left panel shows the momentum transfer to ϕ in the case of a proton target as a function of ϕ production angle. Right panel shows the momentum of a kaon from forward ϕ decay ($\theta^{\phi} = 0$ at 1.1 GeV/c) as a function of opening angle from the beam. Thin lines in both figures are plotted with a step of $\Delta\cos\theta_{CM} = 0.02$.

4.2 Beam Line

The momentum for the incident $\overline{p}$ used the proposed experiment is 1.1 GeV/c. After the consideration, the K1.1 beam line which is now under construction is the best beam line for the proposed experiment. This beam line is designed to have more than 2.0×10^6 $\overline{p}$ per spill beam with 270kW J-PARC PS operation. This means that $\sim10^6$ $\overline{p}$ per spill will be available even J-PARC PS operated with 100 kW. The design of K1.1 spectrometer is shown in Figure 9. Produced $\overline{p}$s at T1 target are separated from other negative particles by DC separators. The momentum of the particle is analyzing by spectrometer magnets. For the momentum analysis and particle identification(PID) in offline analysis, particle tracking chambers are installed before Q8 and after Q11 magnets. Detail of the designed tracking chambers and PID detectors are shown in following sections.

4.2.1 Beam Line Tracker

Trajectory of the incident $\overline{p}$ beam will be tracked with beam line tracker. The momentum of the $\overline{p}$ will be analyzed with this tracking information together with beam optics of beam line magnets. The material in beam line tracker should be minimized, to avoid multiple scattering of incident 1.1 GeV/c $\overline{p}$ beam. Moreover, beam intensity where we are going to install our tracker upstream of the beam line is estimated to be around a few M particles per pulse (0.7s) with proton energy and intensity in J-PARC proton synchrotron as 30 GeV/9μA. It corresponds to a few MHz hit rate. For the

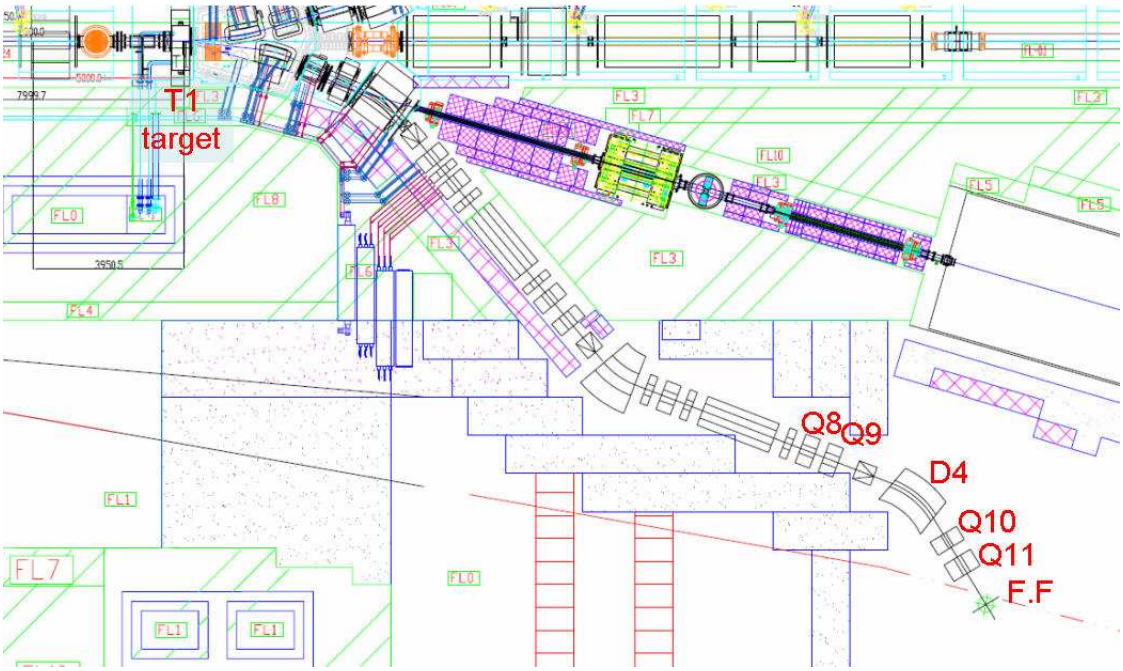

Figure 9: K1.1 beam line.

proposed experiment, planner type of drift chamber with drift cell size of 5 mm is used for the tracking chamber. Six layers of the wire planes are composed as single unit of drift chamber complex (DCC). The wire configuration of a DCC is X-X', U-U', and V-V' where X denoted wire of drift chamber running in vertical, U and V indicate that the wires running with $+30^{\circ}$ and -30° tilted angle respect to X wires, respectively. Four sets of DCCs are installed into the beam line spectrometer.

On the other hand, once upgrade of the 50 GeV PS completed both energy recovery from 30 GeV to 50 GeV operation and beam power upgrade, expected beam rate which tracking chamber need to be handle will be up to 10 MHz. To handle those beam intensity, we also have a upgrade plan of beam line chambers for the detector after beam intensity upgrade, which is tracking detector using Gas Electron Muiliplier (GEM) technique. For example, thickness of the one tracking detector made with GEM is estimated to be $1.0\text{x}10^{-3}$ % radiation length per tracking plain. For the momentum analysis, we need to measure direction of the beam before and after the dipole magnet, so that we need at least 4 tracking planes. Finally, coulomb multiple scattering angle is calculated as 0.7 mrad with 1.0 GeV/c $\overline{p}$. Basic R&D project for the beam line chamber has been started and in progress.

4.2.2 Beam Identification counters

Two type of PID detectors are installed to the beam line spectrometer. One is the beam hodoscope counter, which aimed to identified particles by Time of Flight (ToF) measurement in offline analysis. Two ToF (ToF1 and ToF2) walls, which consists of segmented scintillator counters are installed at the position of before Q8 and after Q11 magnets which is shown in Figure 9. The flight path length is design to have as much as 6m. The ToF counter with resolution of 100 ps, which is easily achievable using the technology at present, is enough to separate $\overline{p}$ of 1.1 GeV/c from other particles, pion and Kaons, with more than 3σ separation.

For the hardware trigger, cherenkov counter to reject contamination of negative pions and Kaons in $\overline{p}$ beam is installed just after ToF2. Figure 10 shows threshold

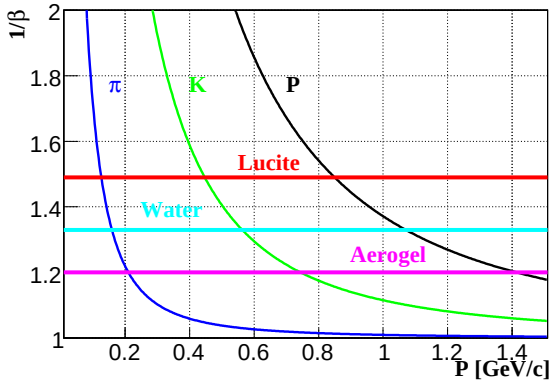

Figure 10: Cherenkov threshold as a function of momentum for pion, kaon and protons.

index(n=1/β) of the each particle species as a function of particle momentum. The figure indicates that to select $\overline{p}$ efficiently, we need to choose cherenkov radiator with refrection index n=1.2. It should be note that recently high dense aerogel done by Chiba Univ. (up to n=1.25) have been developed. The Aerogel with reflection index of n=1.2 is indeed the material which is already available. Therefore we designed Aerogel cherenkov counter with reflection index of n=1.2. Figure 11 shows number of photons expected with n=1.2 Aerogel radiator. As shown in Figure 11, 1.1 GeV/c Pions and Kaons will generate enough cherenkov photons, an order of 140 photons, with 1 cm thick radiator. We will use this Aerogel counter as a VETO counter to purify incident $\overline{p}$ beam. The optimisation of the radiator thickness and optics of the detector system are in progress.

4.3 The target

We propose to use 3 target materials. First one is the Copper target to produce ϕ meson bound state, where mass shift of the ϕ meson have been observed[2]. Second

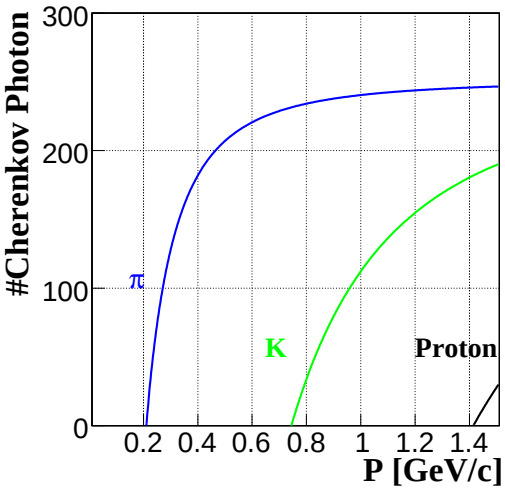

Figure 11: Expected number of cherenkov photons with 1cm, n=1.2 Aerogel radiator.

one is Polyethylene target as a proton target to evaluate elementary production cross section. To evaluate Carbon contribution in Polyethylene target, we also need to take a data with Carbon target. Those three targets, Copper, Carbon and Polyethylene target are used for the measurement. The thickness of the each target material is 2 g/cm^2.

4.4 The spectormeter system

We propose to detect K^+K^- pair from the forward ϕ meson decay, and $K^+\Lambda$ pair from the backward ϕ meson bound state using single spectrometer with large aperture dipole magnet. The spectrometer consist of charged particle tracking system and particle identification counters. The advantage of this detector is wide acceptance for the forward going ϕ meson together with good missing mass resolution from reconstructed particle. The requirement for the spectrometer system are summarized as follows.

1. Forward going K^+K^- pairs from ϕ meson decay must be identified efficiently for online trigger.

2. ϕ meson bound state is identified by missing mass analysis using reconstructed ϕ meson. As discussed in Section 2, the binding energy of the ϕ mesic nucleus are expected to be an order of 30 MeV. For the decay width of the ϕ meson in nucleus, experimentally, it has been reported as $\Gamma_\phi/\Gamma_\phi^{free} \approx 3.4$ [2]. However, theoretically, it has been varied from two to five times bigger than the decay width in vacuum. Now we assume that the decay width of the ϕ meson in nucleus has been five times wider than the decay width in vacuum, which will be $\sim$ 10 MeV(in σ). To distinguish bound state which has binding energy and

width of 30 MeV and 10 MeV, we need to have missing mass resolution of $\leq$ 15-20 MeV/c(σ) . It should be note that if we will be able to accumulate 500 bound state events, it turns out that the resolution of mean peak position of the bound state will be determined with $15/\sqrt{500} \sim 0.7$ MeV/c^2.

3. Final state particles emitted from bound state, K^+ and Λ, need to be identified and detected. This is essential to reduce physical background. Therefore solid angle for the tracking detector need to be large to accumulate enough statistics. And also detector need to have reliable PID capability, especially for Kaons.

The conceptual design for the spectrometer is shown in Figure 12. The target is placed

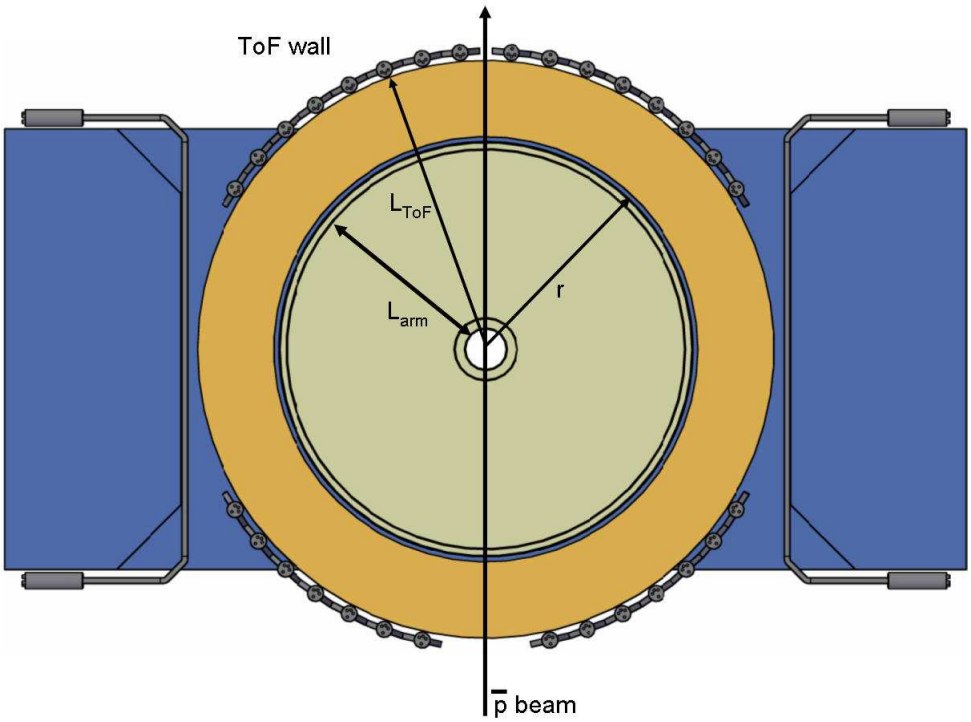

Figure 12: conceptual design for the spectrometer.

on the centre of the dipole magnet. A cylindrical drift chamber(CDC) is surrounding the target to maximize acceptance for the decay particles, namely K^+ and Λ, and forward going Kaons from ϕ meson decay. Around the CDC, ToF wall is installed for the particle identification purpose. Three parameters need to be determined to design the detector, namely, radius of the region where uniform magnetic field will be presented(r), lever arm in the tracking detector(L_{arm}) and the field strength generated by magnet. Those parameter need to be taken to satisfy requirements listed above.

For this proposed experiment, we defined those parameters as following way. The momentum resolution of the CDC can be expressed as follows[19],

$$\delta P = \sqrt{\left(\frac{\delta P_H}{\sin\theta}\right)^2 + \left(P_H \frac{\cos\theta}{\sin^2\theta}\delta\theta\right)^2}, \tag{12}$$

where P_H is the momentum projected onto the plane perpendicular to the direction of the magnetic field expressed by $P_H = Psin\theta$, δP_H is the horizontal momentum resolution, and $\delta\theta$ is the resolution of the angle between the track and the direction of magnetic field. The horizontal momentum resolution is expressed as follows

$$\frac{\delta P_H}{P_H} = \sqrt{\left(\frac{\delta P_H}{P_H}\right)^2_m + \left(\frac{\delta P_H}{P_M}\right)^2_{MS}}, \tag{13}$$

where $(\delta P_H/P_H)_m$ represents resolution from measurement error of spacial position and $(\delta P_H/P_H)_{MS}$ is the effect from multiple coulomb scattering. Each component can be described as follows.

$$\left(\frac{\delta P_H}{P_H}\right)_m = \frac{P_H \sigma_{r\phi}}{0.3L^2B}\sqrt{A_N} \tag{14}$$

$$\left(\frac{\delta P_H}{P_H}\right)_{MS} = \frac{0.05}{\beta B}\sqrt{\frac{1.43}{LX_0}} \tag{15}$$

where

$$\begin{aligned}
\sigma_{r\phi} &= \text{spacial resolution in the } r-\phi \text{ plane per wire (m)} \\
L &= \text{lever arm length (m)} \\
B &= \text{magnetic field (T)} \\
A_N &= \frac{720}{N+5}\text{where N is the number of sampling points} \\
\beta &= \text{velocity of the particle} \\
X_0 &= \text{radiation length of chamber gas.}
\end{aligned} \tag{16}$$

The over all angular resolution $\delta\theta$ is given as,

$$\delta\theta = \sqrt{(\delta\theta)^2_m + (\delta\theta)^2_{MS}} \tag{17}$$

where each components are given as follows.

$$(\delta\theta)_m = \frac{\sin^2\theta}{L_{arm}}\delta_V \tag{18}$$

$$(\delta\theta)_{MS} = \frac{0.015}{p\beta c}\sqrt{\frac{L_{arm}}{X_0}} \tag{19}$$

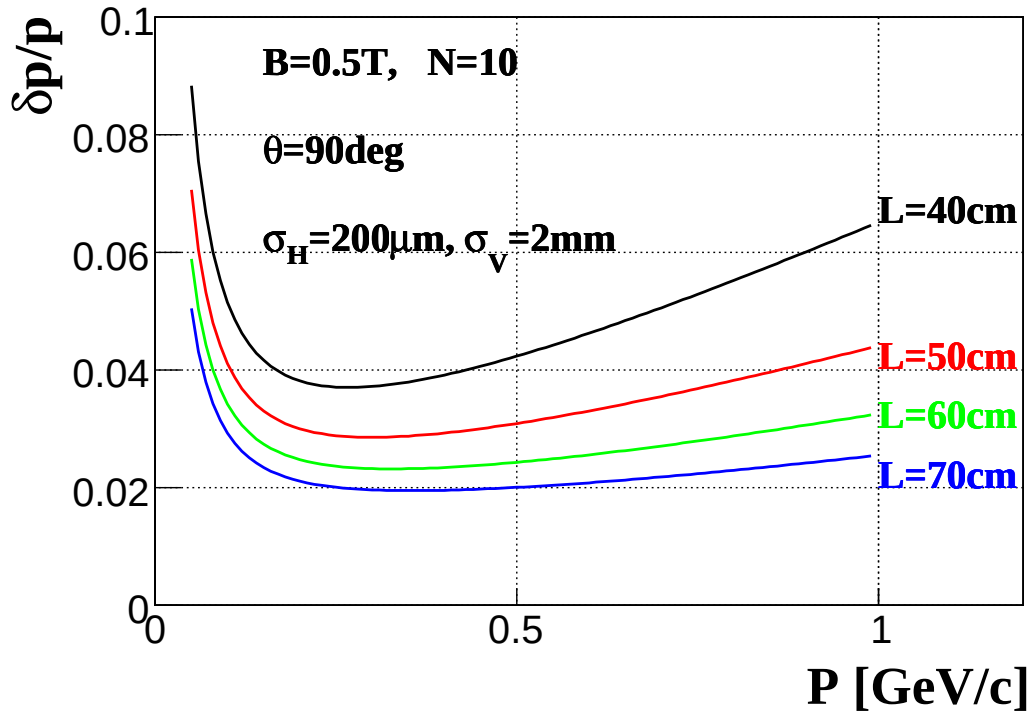

Figure 13: momentum resolution as a function of the momentum, with different lever arm (L_{arm}) of the tracking detector

where, δ_V is spacial resolution of $Vertical$ coordinate(parallel to the magnetic field), L_{arm} is an arm length of measurement points. Figure 13 shows total momentum resolution as a function of the arm length. Using results obtained above evaluation, we estimated missing mass resolution of the ϕ meson bound state using reconstructed forward going ϕ meson as a function of L_{arm} and strength of magnetic field. The result is tabulated in Table 2, where 2.0 g/cm^2 of Carbon is used for the target material. To achieve required resolution, we need to construct CDC with L_{arm} more than 50 cm with B$\sim$0.5 T magnet.

L_{arm} (cm) / B (T)	40	50	60	70
0.4	32. MeV/c^2	25. MeV/c^2	19. MeV/c^2	16. MeV/c^2
0.5	26. MeV/c^2	20. MeV/c^2	15. MeV/c^2	13. MeV/c^2
0.6	22. MeV/c^2	16. MeV/c^2	13. MeV/c^2	11. MeV/c^2

Table 2: Expected missing mass resolution

The design of the Time of Flight wall is done as follows. For the proposed experiment, we need to detect short-lived Kaons at relatively low momentum. Therefore,

ToF needs to be placed as close as possible from the target to minimise decay loss of Kaons. The distribution of the Kaons emitted from both forward and backward ϕ meson are shown in Figure 14. The Kaons with momentum between 200 MeV/c to 600 MeV/c need to be identified with this ToF wall. For this consideration, the ToF wall is placed 100 cm away from the target to secure L_{arm}=50 cm for the CDC.

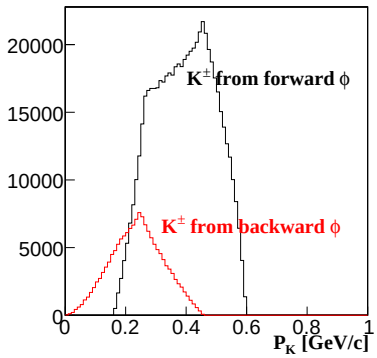

Figure 14: Momentum distribution of forward and backward Kaons.

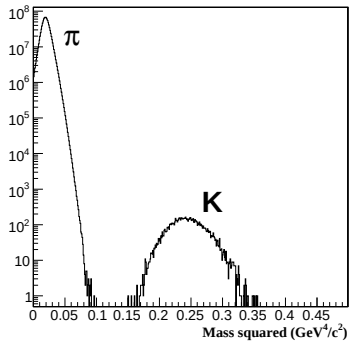

Figure 15: Mass squared distribution for the particle with momentum 200 MeV/c < 400 MeV/c.

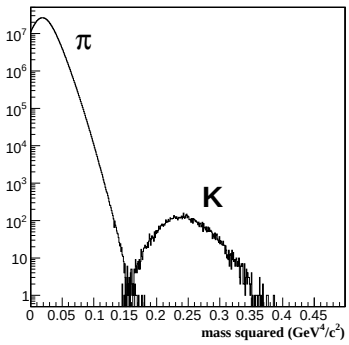

Figure 16: Mass squared distribution for the particle with momentum 400 MeV/c < 600 MeV/c.

Now we start to evaluate PID capability of the ToF wall. Figure 15 and Figure 16 shows mass squared distribution calculated from ToF, with the particle momentum 200 MeV/c <p<400 MeV/c and 400 MeV/c <p<600 MeV/c, respectively, with assumed ToF resolution of 100 ps and π/K ratio about 10^5. Figures show that ToF wall with 100 ps resolution achieved more than 2 σ separation of pion and kaons. Recently, new-type ToF wall, Resistive Plate Chamber (RPC) has been successfully developed and applied in various experiments. One of the group reported that they achieved intrinsic timing resolution of the counter as 25 ps. Big advantage for the ToF wall with RPC is that the detector works fine even in high magnetic field environment. Therefore, ToF wall constricted with RPC is a choice for proposed experiment. Basic R&D to use RPC is now started.

As we discussed in Section 3.5, requirement of two Kaons in the forward direction is essential to reduce fake trigger rate. It should be note that large interaction cross section for the $\overline{p}$p reaction may produce more than 100 kHz triggers if we only required two charged tracks in forward direction. As we can see in Figure 14, the momentum range where we need to identify in trigger level is 250 MeV/c to 700 MeV/c. For this purpose, cherenkov trigger counter is installed only in the forward direction. As shown in Figure 10, the best choice of reflection index of the radiator is n=1.2, which is also proposed to use as cherenkov radiator for beam line spectrometer.

4.5 Yield estimation and beam time request

The number of the expected yield can be estimated as follows.

$$Y = I_{\overline{p}} \times L/A \times N_A \times \sigma_{\overline{p}^A_Z X} \times \epsilon_F \times \epsilon_{Decay} \times P_{sticking} \times \epsilon_{Analysis}, \tag{20}$$

where, $I_{\overline{p}}$ is $\overline{p}$ intensity per spill, L is Target thickness in g/cm^2, A is the mass number of target nucleus N_A is the Avogadro number, $\sigma_{\overline{p}^A_Z X}$ is production cross section ϵ_F is trigger efficiency for forward going kaons, ϵ_{Decay} is the acceptance of decay particles from bound state, $P_{sticking}$ is sticking probability of the ϕ meson, $\epsilon_{Analysis}$ is DAQ and analysis efficiency. Those numbers are estimated as follows.

The $(\overline{p}, \phi)$ experiment is limited by the incident $\overline{p}$ beam rate, even at J-PARC. The maximum $\overline{p}$ intensity is expected to be about $I_{\overline{p}} = 1.0 \times 10^6$ per spill at 30 GeV/100 kW operation of the proton synchrotron evaluated by empirical Sanford-Wang formula. ‡

Measurements of ϕ meson production cross section by p($\overline{p}$,ϕ)ϕ reaction is available for incident beam momentum above 1.2 GeV/c. To evaluate production cross section above production threshold, 0.86 GeV/c, to 1.2 GeV/c, we assumed that the evolution of the ϕ meson production cross section is to be a power function of the excess energy from threshold energy, *i.e.* $\sigma = C \times (\sqrt{s} - \sqrt{s_0})^{-1/2}$, where C is free parameter. We fitted the existing data with the formula evaluated cross section below 1.2 GeV/c is shown in Figure 17. From the Figure 17, we can expect 2.4 μb at 1.1 GeV/c. In the

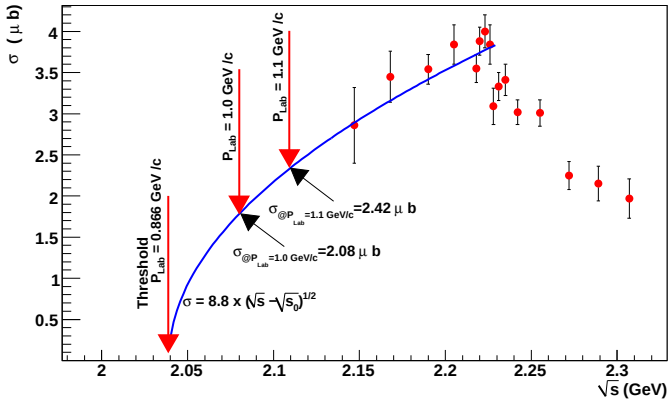

Figure 17: Estimated production cross section near the production threshold.

case of $\overline{p}$-nucleus collisions, we assumed that the dependence of the total cross section will be number of protons in nucleus (Z) lather than mass number (A). Therefore, we use $\sigma_{\overline{p}^A_Z X} = Z^{2/3} \times \sigma_{\overline{p}p}$. The geometrical acceptance of the forward ϕ meson ϵ_F is evaluated by simple Monte Carlo(MC) simulation and get 1.5×10^{-1} including in flight decay of Kaon.

‡J-PARC proton synchrotron (50 GeV-PS) will be operated at a repetition rate of 3.52 seconds, providing a slow extraction period of 0.7 sec (*spill*).

As we discussed in section 3.1.3, we need to evaluate sticking probability of the ϕ meson to the nucleus($P_{sticking}$). Because of wide acceptance of the forward detector, triggered ϕ meson will have rather broad momentum distribution. To evaluate appropriate sticking probability, we need to take into account momentum distribution of the accepted ϕ mesons which is shown in Figure 18. Final averaged sticking probability is

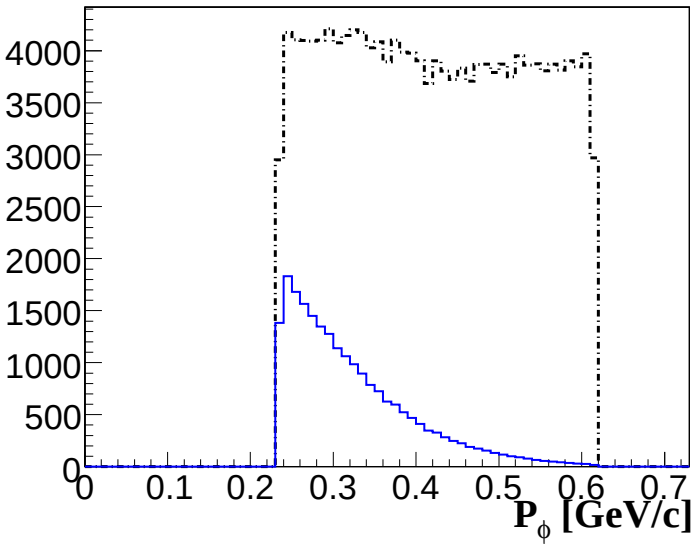

Figure 18: Momentum distribution of backward ϕ meson. Broken line shows momentum distribution of trigger accepted ϕ meson, solid line shows ϕ meson momentum distribution of trigger accepted ϕ meson together with the sticking probability which is discussed in section 3.1.3.

estimated to be 0.13.

Acceptance of the decayed particles (ϵ_{Decay}) form the bound state and the particle produced at elementary process are different. The decay particles produced from the bound state, K^+ and Λ, will be emitted isotropic. On the other hand, the particle produced at elementary process (K^+ and K^-) will be forward boosted. Those effect is also evaluated with simple MC simulation and found to be 0.056 and 0.08 for the case of bound state formation and elementary process, respectively. In addition, decay branching ratio of $\Lambda \to \pi^- p$ is included to the event rate estimation in case of bound state production. Finally, the DAQ and Analysis efficiency ($\epsilon_{Analysis}$) is assumed to be 0.7. The number used for the estimation and the resultant event numbers are tabulated in table 3. As shown in the table, we can expect to observe $\sim$ 330 and 600 events of the ϕ meson formation on Cu and C target respectively within 120 shifts at $\overline{p}$ intensity of 1×10^6 / *spill*. Thanks to the lower momentum transfer (quasi-recoilless condition) of the $(\overline{p}, \phi)$ reaction, we obtained an excellent formation rate despite the lower cross section.

Target		Cu	Carbon	$H_{Polyethylene}$
$\overline{p}$ intensity (/spill)	$I_{\overline{p}}$	10^6	10^6	10^6
mass number	A	63.5	12.0	1.
charge number	Z	29	12	1
cross section ($Z^{2/3} \times \sigma_{\overline{p}p}$) ($\mu b$)	$\sigma_{\overline{p}^A_Z X}$	23.	7.9	2.4
Target thickness (g/cm^2)	L	2.0	2.0	2.0
Acc. for Forward Spectrometer	ϵ_F	1.5×10^{-1}	1.5×10^{-1}	1.5×10^{-1}
Acceptance for decay particle	ϵ_{Decay}	0.056	0.056	0.08
Averaged Sticking probability	$P_{sticking}$	0.13	0.13	(N/A)
Analysis and DAQ efficiency	$\epsilon_{Analysis}$	0.7	0.7	0.7
expected yield/spill		3.4×10^{-4}	6.3×10^{-4}	3.6×10^{-3}
expected yield/shift		~ 2.8	~ 5.1	$\sim 29.$
expected yield/120 shift		~ 330	~ 600	~ 3400

Table 3: Expected event rate

In summary, we propose to taking data with two conditions. First physics run is with carbon and polyethylene target simultaneous for 120 shifts. And the other run is taking data with only copper target for 120 shifts. In total, 240 shifts are requested for the proposed experiment.

4.6 Trigger condition and signal/background ratio

The main trigger for the experiment is two kaons in forward detector together with $\overline{p}$ beam identified by beam line counters.

When we equipped reflection index (n=1.2) aerogel as a radiator of cherenkov counter for forward spectrometer, most of the pion background is suppressed. Because expected number of photon emitted by expected background pions with 1 cm Aerogel counter is $\sim$ 50-100 photons, where Kaon is below the threshold. Here we assumed pion rejection factor for the Aerogel counter is to be 10^{-2}. For the trigger condition, charged particle hits on forward ToF wall together with Aerogel counter information is required. In the multi-pion production events, not only charged pions but also π^0 will be produced. Gammas from π^0 decays will also be a source of possible background on hardware trigger level. If we assume detection efficiency of single gamma by ToF wall to be 10% therefore fake trigger rate generated by $\pi^0 \to 2\gamma$ is to be 1%. Thus, the number of expected background trigger rate for each possible background sources for Copper target are tabulated in Table 4. As shown in Table 4, we expect the fake trigger rate to be about 690 per spill. It should be note that those background mist be vanished in the offline analysis, once we required K^+ emission from the target.

Process	σ_{Total} (mb)	Two hits on Forward Trigger counters	# of trigger /spill
signal	$23.\times10^{-3}$	0.3	4.3×10^{-1}
$\pi^+\pi^0\pi^-$	33.	5.0×10^{-3}	3.1
$2\pi^+2\pi^-$	47.	5.0×10^{-3}	4.1
$\pi^+2\pi^0\pi^-$	14.	2.0×10^{-2}	5.2
$2\pi^+\pi^02\pi^-$	224.	3.1×10^{-2}	130.
$2\pi^+2\pi^02\pi^-$	125.	8.0×10^{-2}	190.
$3\pi^+3\pi^-$	18.	7.4×10^{-2}	25.
$2\pi^+3\pi^02\pi^-$	86.	1.5×10^{-1}	240.
$2\pi^+4\pi^02\pi^-$	22.	2.2×10^{-1}	90.
		sum of all contributions	$\sim$ 690

Table 4: Estimated trigger rate of possible background source

5 Cost estimate and schedule

5.1 Cost of the experiment

Summary of the cost estimation for the proposed experiment is shown in Table 5. For the proposed experiment, all components except spectrometer magnet need to be constructed. In total, 128 M yen is required to construct proposed experiment. It should be note that as shown in Table 5, DAQ system takes up major portion of the budget. Therefore reduction of the total cost will be possible to use DAQ system which is already exist, like KEK-VME system.

5.2 Time schedule

Detail time line for the proposed experiment is shown in Figure 19. As shown in the figure, we are intended to complete all preparation for the detector construction by end of calendar year 2013.

References

[1] R. Arnaldi *et al*, Phys. Rev. Lett. **96**, (2006) 162302.

[2] R. Muto *et al.*, Phys. Rev. Lett. **98** (2007) 042501.

[3] G. E. Brown and M. Rho, Phys. Rev. Lett. **66** (1991) 2720-2723.

[4] T. Hatsuda and S. H. Lee, Phys. Rev. **C46** (1992) 34-38.

[5] T. Hatsuda, H. Shiomi and H. Kuwabara, Prog. Theor. Phys. **95** (1996) 1009-1028.

Item		cost [JPY]
Beam Line		
	Beam line tracker	10M
	Beam line ToF counter	8M
	electronics	5M
Main Spectrometer		
	spectrometer magnet	-
	Cylindrical drif chamber(CDC)	30M
	CDC electronics	15M
	ToF wall	10M
	Aerogel Cherenkov counter	10M
DAQ system		
	ADC, TDC etc.	30M
miscellaneous items		
	cables, maintenance cost, etc.	10M
Total		128M

Table 5: Cost estimation

[6] F. Klingl, T. Waas and W. Weise, Phys. Lett. **B431** (1998) 254-262.

[7] E. Oset and A. Ramos, Nucl. Phys. **A679** (2001) 616-628.

[8] T. Yamazaki and Y. Akaishi, Phys. Lett. **B453** (2000) 1-6.

[9] H. Geissel *et al.*, Phys. Rev. Lett. **88** (2002) 122301.

[10] K. Suzuki *et al.*, Phys. Rev. Lett. **92** (2004) 072302.

[11] T. Suzuki *et al.*, Phys. Lett. **B597** (2004) 263.

[12] M. Iwasaki *et al.*, arXiv: arXiv:0706.0297 to be appeared in EPJ.

[13] M. Agnello *et al.*, Phys. Rev. Lett. **94**, (2005) 212303.

[14] T. Kishimoto *et al.*, Prog. Theo. Phys. **118** (2007) 181

[15] F. Klingl, T. Waas and W. Weise, Phys. Lett. B **431** (1998) 254.

[16] E. Oset *et al.*, Acta Phys. Hung. A **27** (2006) 115.

[17] S. Yokkaichi *et al.*, J-PARC E16 proposal,
http://j-parc.jp/NuclPart/pac_0606/pdf/p16-Yokkaichi_2.pdf

[18] C. Evangelista *et al.*, Phys. Rev. D57(1996) 5370.

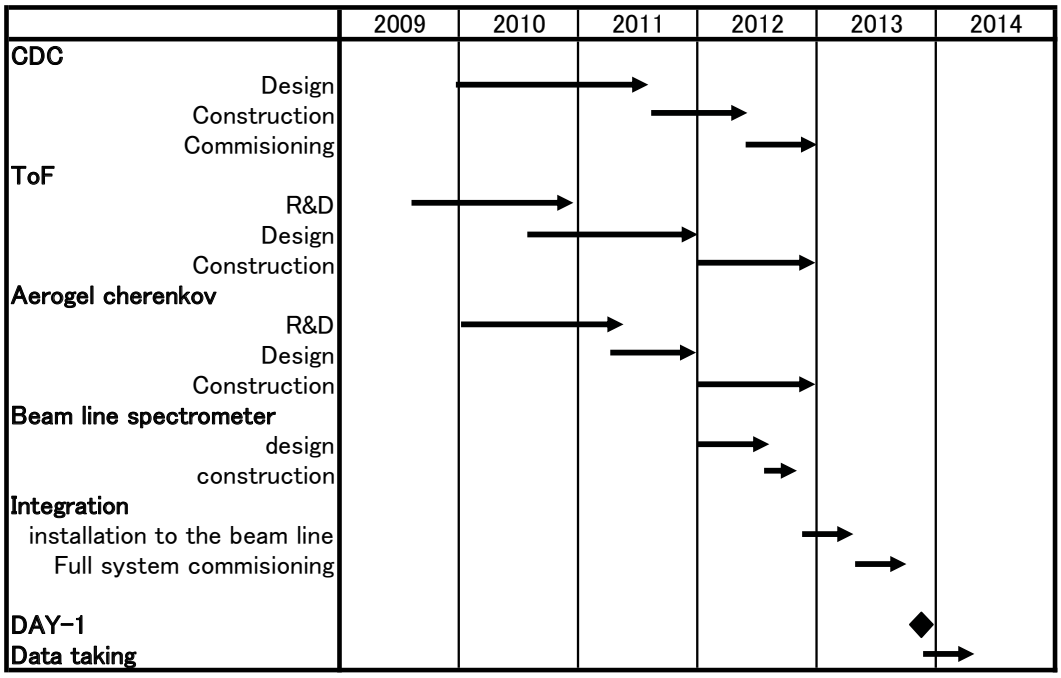

Figure 19: Proposed time schedule of the experiment

[19] R. Gluckstern, Nucl. Inst. Meth. 24 (1963) 381